Science of the Total Environment 787 (2021) 147683

Contents lists available at ScienceDirect

Science of the Total Environment

journal homepage: www.elsevier.com/locate/scitotenv

The impact of different types of high surface area brush fibers with different electrical conductivity and biocompatibility on the rates of methane generation in anaerobic digestion

Gahyun Baek [a], Ruggero Rossi [a], Pascal E. Saikaly [b], Bruce E. Logan [a,*]

[a] Department of Civil and Environmental Engineering, The Pennsylvania State University, 231Q Sackett Building, University Park, PA 16802, USA
[b] Biological and Environmental Science and Engineering Division, Water Desalination and Reuse Research Center, King Abdullah University of Science and Technology, Thuwal, Saudi Arabia

HIGHLIGHTS

- Fibers with different surface characteristics were added in anaerobic digesters.
- Only the polyester-added reactors showed the lowest methane production.
- Higher biomass was detected in the biocompatible horsehair and carbon brushes.
- Electrical conductivity alone may not enhance anaerobic digestion performance.
- Biocompatibility should be considered in the conductive materials-added studies.

GRAPHICAL ABSTRACT

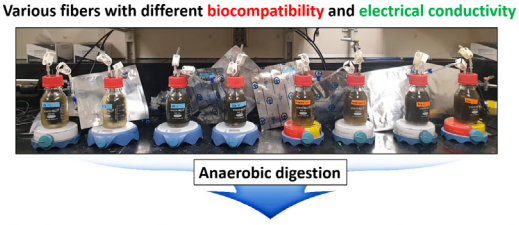

	Biocompatibility	Electrical conductivity	Brush materials	Methane production (mL/g COD_{fed})
1	Good	Good	Carbon fiber	85
2	Good	Poor	Horsehair	84
3	Poor	Good	Stainless steel fiber	80
4	Poor	Poor	Polyester fiber	68

ARTICLE INFO

Article history:
Received 13 April 2021
Received in revised form 6 May 2021
Accepted 6 May 2021
Available online 11 May 2021

Editor: Yifeng Zhang

Keywords:
Anaerobic digestion
Biocompatibility
Electrical conductivity
Microbial community structure
Surface area

ABSTRACT

The addition of electrically conductive materials may enhance anaerobic digestion (AD) efficiency by promoting direct interspecies electron transfer (DIET) between electroactive microorganisms, but an equivalent enhancement can also be achieved using non-conductive materials. Four high surface area brush materials were added to AD reactors: non-conductive horsehair (HB) and polyester (PB), and conductive carbon fiber (CB) and stainless steel (SB) brushes. Reactors with the polyester material showed lower methane production (68 ± 5 mL/g COD_{fed}) than the other non-conductive material (horsehair) and the conductive (graphite or stainless steel) materials (83 ± 3 mL/g COD_{fed}) ($p < 0.05$). This difference was due in part to the higher biomass concentrations using horsehair or carbon (135 ± 43 mg) than polyester or stainless steel or materials (26 ± 1 mg). A microbial community analysis indicated that the relative abundance of electroactive microorganisms was not directly related to enhanced AD performance. These results show that non-conductive materials such as horsehair can produce the same AD enhancement as conductive materials (carbon or stainless steel). However, if the material, such as polyester, does not have good biomass retention, it will not enhance methane production. Thus, electrical conductivity alone was not responsible for enhancing AD performance. Polyester, which has been frequently used as a non-conductive control material in DIET studies, should not be used for this purpose due to its poor biocompatibility as shown by low biomass retention in AD tests.

* Corresponding author.
E-mail address: blogan@psu.edu (B.E. Logan).

https://doi.org/10.1016/j.scitotenv.2021.147683
0048-9697/

1. Introduction

Anaerobic digestion (AD) is an established and effective method for wastewater treatment and biogas production. However, due to the slow growth rates of methanogens and imbalanced syntrophic relationship between organic-oxidizing bacteria and methanogens, long residence times are usually required for stable and efficient operation of AD. Adding conductive materials to stimulate direct interspecies electron transfer (DIET) has been shown to be an effective way to enhance AD efficiency (Baek et al., 2018; Lovley, 2017; Yin and Wu, 2019). DIET is an alternative route to indirect interspecies electron transfer (IIET) based on redox mediators (i.e. H_2 and formate) (Baek et al., 2018). DIET is also energetically more advantageous than IIET due to unnecessariness of several enzymatic steps to produce mediators (Lin et al., 2017). Various conductive materials have been implicated to promote DIET including carbon fibers, granular activated carbon, magnetite, and biochar based on the resulting significant increase in methane generation rates and overall process stability (Baek et al., 2017; Jia et al., 2020; Park et al., 2018; Wang et al., 2021). The existence of DIET in these systems was mainly supported by the enrichment of electroactive bacteria and methanogens in the presence of these electrically conductive materials.

The addition of any type of particles or materials can also increase biomass retention inside digesters by providing large amounts of surface area. Adding high surface area is known as an efficient method to enhance biofilm development and thus increase solid retention time (SRT) while minimizing biomass washout (Liu et al., 2020b; Najafpour et al., 2006; Yan et al., 2020). Microorganisms can adhere to the surface of inert supporting media such as granular activated carbon, porous foams, and zeolite (Poirier et al., 2017; Yang et al., 2004). Most of the conductive materials used to promote DIET have large surface areas, making it difficult to untangle the separate effects of surface area and conductivity. Carbon-based conductive materials also usually have porous and entangled structures that provide both high surface areas for microbial attachment as well as hydrophilic and biocompatible surface properties that promote bacterial adhesion (Bian et al., 2018). Due to these surface areas and biocompatibility properties of materials, it is possible that benefits from conductive material addition could be derived not only from the electrical conductivity but also from high biomass retention effect.

The separate impacts of electrical conductivity and surface area of added materials have not been adequately addressed in previous studies due to a lack of suitable controls for both surface area and biocompatibility (Lei et al., 2019; Park et al., 2018; Wang et al., 2021; Zhao et al., 2016). For example, biochar was added as a DIET stimulant in the up-flow sludge blanket reactor (UASB) with >1000 m^2 of Brunauer-Emmett-Teller (BET) surface area, while control reactors had no particles (Zhao et al., 2016). Similarly, methane production rates was increased by 17–19% from propionate and butyrate in reactors containing graphite felt compared to a control without any other materials (Zhang et al., 2019). Adding powdered or granular activated carbon also significantly enhanced performance of AD compared to controls without those materials (Park et al., 2018). In several studies, the effects of adding electrically conductive materials have been compared to controls containing polyester cloth (Dang et al., 2016; Dang et al., 2017; Jia et al., 2020). However, it was not shown that polyester was a suitable control because it could also have poor biocompatibility for biofilm growth. Characteristics of the materials that include roughness, hydrophilicity, and surface energy can also impact bioadhesion availability and thus biomass retention in the reactor (Al-Amshawee et al., 2020; Yuan et al., 2018). In a recent study examining enhanced AD using a microbial electrolysis cell (MEC), two different carbon materials were tested as biocathodes, a graphite plate and a carbon brush, to examine the impact of surface area, but it could not address the importance of DIET for those two materials (Liu et al., 2020a). Therefore, the use of additional controls is needed to fully address biocompatibility, surface area and electrical conductivities of materials.

The hypothesis of this study was that the biocompatibility of the materials is as important as the electrical conductivity of the materials in increasing AD performance. To prove this hypothesis, four different fiber materials (i.e., carbon, stainless steel, horsehair, and polyester) which differed in their electrical conductivity and biocompatibility were used in AD tests to determine their impact on methane generation rates and overall reactor performance. AD performance in each configuration as well as microbial community structure were investigated along with physicochemical analyses of each fiber.

2. Materials and methods

2.1. Reactor construction

Lab-scale anaerobic digesters were constructed with glass bottles filled with 270 mL of liquid volume and containing 80 mL of headspace. Each bottle had two ports to connect the headspace to a biogas collection bag (Cali-5-Bond, Calibrated Instruments, NY) and to collect liquid samples from the middle of the reactors. The bottles were tightly sealed with a rubber stopper and a screw cap (Fig. 1A). Each reactor had a brush almost completely occupying the reactor volume to maximize surface area effect (Baek et al., 2021). All brushes had the same encased volume (6 cm long and 4 cm in diameter, encased volume of 75 mL) but were made with four different fiber materials wound into two twisted titanium wires (Mill-Rose, USA). The wires were held in place by piercing the end through a rubber stopper at the top, and the connection was sealed with epoxy. The brush materials were carbon fiber (CB; Zoltec), stainless steel fiber (SB; stainless steel 304; Loos&Co.), horsehair fiber (HB; Mill-Rose), and polyester fiber (PB; Mill-Rose) to create a different environment for biofilm acclimation by different extent of electrical conductivity and biomass adhesion availability (Fig. 1B). The impact of electrical conductivity was assessed by comparing two non-conductive materials made of horsehair or polyester (used in many DIET tests as a non-conductive control), with carbon and stainless steel which both have high electrical conductivity. The detailed properties such as the fiber diameter, numbers of fibers used to make a brush, and specific total bristle areas are listed in the supporting information (Fig. S1). Carbon fibers had a much smaller diameter and thus a higher number of fibers than the other materials due to a lack of availability of these other materials with this smaller size. The specific bristle area (A_s) of brushes was estimated based as $A_s = 2\ m/r\rho$, where m is the total mass of the bristles of a brush, r is the radius of bristle, and ρ is the density of each fiber. However, many of the individual fibers are grouped together (Fig. 1B) so that this calculated bristle area likely overestimated the available surface area of the materials. A previous study that examined the effect of current generation on AD performance showed that a large graphite brush with no current produced more methane than a reactor with a small brush in the absence of current generation (Baek et al., 2021). Therefore, a control lacking a brush was not used in the current study as the biomass in the reactor would be washed out due to the large amount of medium exchange in each repeated cycle, and it would not produce methane efficiently.

2.2. Reactor operation

A synthetic substrate was used for AD tests containing glucose as the sole carbon source (2.5 g/L) in 100 mM phosphate buffer solution (PBS) containing 4.9 g/L $NaH_2PO_4 \cdot H_2O$, 9.2 g/L Na_2HPO_4, 0.6 g/L NH_4Cl, 0.3 g/L KCl, mineral (12.5 mL/L) and vitamin (5 mL/L) solutions (pH =7.1, conductivity = 13.0 mS/cm). Sludge was collected from the anaerobic digester at the Pennsylvania State University wastewater treatment plant and used as the inoculum after being sieved using a screen (mesh size of 850 μm). The characteristics of the anaerobic sludge inoculum were: total chemical oxygen demand (COD) of 22,500 ± 500 mg/L, soluble COD (SCOD) of 540 ± 30 mg/L, total suspended solids

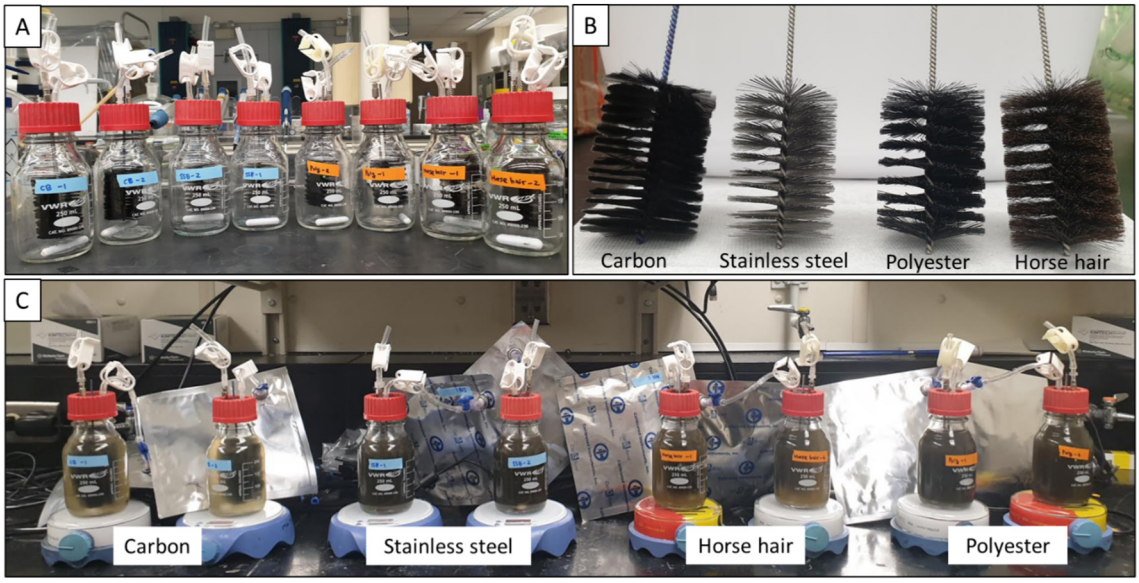

Fig. 1. (A) Schematics of the AD reactor configurations, (B) photographs of the brushes made of different fiber materials, and (C) photographs of reactor operation.

(TSS) of 19,000 ± 700 mg/L, and a volatile suspended solid (VSS) of 14,800 ± 400 mg/L.

The anaerobic reactors were operated in fed-batch mode. At the initial point of the experiment, 20% (*v*/v) of inoculum was added to medium containing glucose with final concentration of 2.5 g/L. At the end of every batch cycle, 50% of medium was removed through sampling port and refilled with fresh medium while the reactor solution was continuously mixed using a magnetic stir bar. Prior to each cycle, the replaced medium was sparged with nitrogen gas for 3 min to remove residual gas in solution and headspace and make anaerobic environment. The batch cycles were repeated four times during total 51 days of operational period and data of the last batch cycle was presented. During acclimation period, only biogas amount was monitored without analyzing biogas composition (Fig. S2). All reactors were run in duplicate and maintained at 35 °C in a temperature-controlled room or incubator. The biogas and liquid samples were collected and analyzed every 2–5 days depending on the rate of AD process.

2.3. Protein quantification

Total protein concentration of the suspension and biofilm were quantified by a bicinchoninic acid (BCA) protein assay kit (Sigma Aldrich) following a previous method (Bond and Lovley, 2003; Ishii et al., 2008). The attached biomass onto the fibers were extracted using 0.2 N NaOH. First, the pieces of brushes were cut with sterile scissors and placed in a petri dish with 5 mL of 0.2 N NaOH. The extraction was performed for 1 h at 4 °C by flushing NaOH solution several times over the surface of brushes using pipette every 15 min to improve extraction efficiency. The solution was removed after 1 h and weighed. An equal amount of deionized water was used to further rinse the brushes to collect any remaining solution. The liquids (i.e., equal amount of 0.2 N of NaOH and deionized water) were pooled together, yielding a sample containing 0.1 N NaOH. For suspended biomass, 10 mL of mixed liquor was centrifuged at 13,000 ×*g* for 3 min, the suspension was removed, and the pellet was re-suspended in 5 mL of 0.1 N NaOH. For cell lysis, a freeze-thaw cycle was repeated three times at −20 °C for freezing and 100 °C for thawing both biofilm- and suspension-derived samples. The pretreated sample was centrifuged (13,000 ×*g*, 3 min) to remove any cell debris and the protein assay was performed by the BCA method against a bovine serum albumin standard. The measured protein was normalized by the weight of used fibers (for attached biomass) or the volume of used suspension (for suspended biomass). Total protein in each reactor was finally estimated by multiplying by the total weight of fibers or the total liquid volume of the reactor.

2.4. Scanning electron microscopy

The surface morphology of raw fibers and collected fibers at the end of the fourth cycle was analyzed by scanning electron microscopy (SEM). For the fibers with biofilm, pretreatment method was used to fix and dehydrate cell structures following a previous procedure (Baek et al., 2020). First, small pieces of fibers were cut using sterile scissor and washed three times with phosphate-buffered saline (10 mM of phosphate buffered saline, pH 7.4) and fixed in 2.5% glutaraldehyde solution for 4 h at 4 °C, followed by washing three times with phosphate-buffered saline. The fibers were dehydrated with serial steps with 50%, 70%, 90%, and 100% of ethanol at room temperature for 15 min per each step. The samples were air-dried overnight and analyzed with SEM (Verios G4, Thermo-Scientific, Hillsboro, OR). The secondary electron images were obtained using an accelerating voltage of 3 or 5 keV depending on the magnification.

2.5. Chemical analyses and calculations

COD concentrations were analyzed using standard methods (TNTplus COD reagent; HACH company). Volatile fatty acids (VFAs; acetate, propionate, and butyrate) were analyzed using a gas chromatograph (GC; Shimadzu, GC-2010 Plus, Japan) equipped with a Stabilwax-DA column (30 m × 0.32 mm × 0.5 μm, Restek, Bellefonte, PA) and flame ionization detector (FID; a detection limit of each VFAs of 0.1 mM) with nitrogen as the carrier gas. The samples for both SCOD and VFA measurement were filtrated using a syringe filter with 0.45 μm of pore size. The total and suspended solid concentrations were measured according to a standard method (WEF, 2005). The gas composition in the headspace of the reactors was analyzed with a GC (SRI Instrument, Torrance, CA, USA) using 250 μL of gas from the gas collection bag using an airtight gas syringe (Hamilton, Reno, NV, USA). H_2 and CH_4 were analyzed using a GC (model 2601B, SRI Instrument, Torrance, CA, USA) equipped with thermal conductivity detector (TCD; a detection limit of 0.01%) and a 3-m Molsieve 5A 80/100 column (Altech Associates, Inc., Bannockburn, IL) with argon as the carrier gas. CO_2 was analyzed using another GC (model 310, SRI Instrument, Torrance, CA, USA) with TCD (a detection limit of 0.01%) and a 1-m silica

gel column (Restek, Bellefonte, PA, USA) with helium as the carrier gas. The methane volume at time t was calculated as $V_{m,t} = V_{g,t} f_{m,t} + V_h (f_{m,t} - f_{m,t-1})$,where $V_{g,t}$ is biogas volume in gas bag and $V_{m,t}$ is methane volume (mL), f_m is the fraction of the methane in total biogas, and V_h is the headspace volume (mL) of the reactor. Because there was a gas leakage problem in one of the duplicates of HB reactor, the theoretical methane accumulation was calculated based on the SCOD consumption profile only for one of the HB reactors, then averaged with measured methane production of another HB reactor. The volume was corrected to standard condition (0 °C and 1 atm). The samples for analyses were extracted from both duplicate reactors and all chemical analyses were conducted in duplicate.

2.6. Next-generation sequencing

The biomass samples were collected from the attached biofilm on the brushes and mixed liquor of each reactor at the end of the experiment. RNA was extracted using the standard protocol for RNeasy PowerMicrobiome Kit (Qiagen, Germany) and then reverse-transcribed using 2× Platinum SuperFi RT-PCR Master Mix from the SuperScript IV One-Step RT-PCR System (Thermo Fisher Scientific, USA). The 16S rRNA sequencing libraries were prepared according to the Illumina protocol by using the forward (515F) and reverse (806R) tailed primers (Apprill et al., 2015; Illumina, 2015). The detailed information about sequencing and data processing procedures are described in the previous paper (Baek et al., 2021). The sequences obtained in this study were deposited in the NCBI Sequence Read Archive under the Bioproject accession number PRJNA699668. Clustering analysis was performed based on the Sorensen distance measurement based on the recommendation for ecological community data analysis (McCune et al., 2002).

3. Results & discussion

3.1. Anaerobic digestion performance

After three repeated fed-batch cycles for acclimation of microbial community to each experimental condition, biogas volume and composition were analyzed during the fourth cycle. During 18 days of operation, a significantly higher rate of methane production was observed for the reactors with the horsehair, carbon, and stainless steel brushes than those with the polyester brush ($p < 0.05$; days 4–18) (Fig. 2A). The final volume of methane gas accumulation was 83 ± 3 mL/g COD_{fed} while the polyester brush reactor produced only 68 ± 5 mL/g COD_{fed}. In terms of SCOD removal efficiency. Similar patterns were shown by much faster organic degradation in the horsehair, carbon, and stainless steel brush reactors (174–190 mg COD/L·d until day 10) compared to the polyester brush reactor (129 ± 0 mg COD/L·d until day 10) (Fig. 2B). Taken together, these data indicated that the performance with the non-conductive horsehair brush was the same as the electrically conductive carbon and stainless steel brushes, and therefore that electrical conductivity of the material was not required to achieve enhanced performance. The non-conductive polyester brush performance was worse than the horsehair brush, suggesting that polyester was not a good material as a control for a non-conductive material. The stainless steel brush reactor had methane production and SCOD removals similar to those of the carbon brush, so it was not clear based only the methane generation and SCOD removal rates if electrical conductivity was helpful in the case of this material.

In the initial phase of a batch cycle (days 2–7), the stainless steel brush reactor exhibited slightly lower methane production and SCOD removal rates, but it showed a more rapid AD rate after day 7 which was comparable to performances of carbon and horsehair brush reactors. The changes in methanogenic rate observed using the stainless steel brush reactor were presumably due to the surface properties of stainless steel fiber which have been shown to be much less compatible

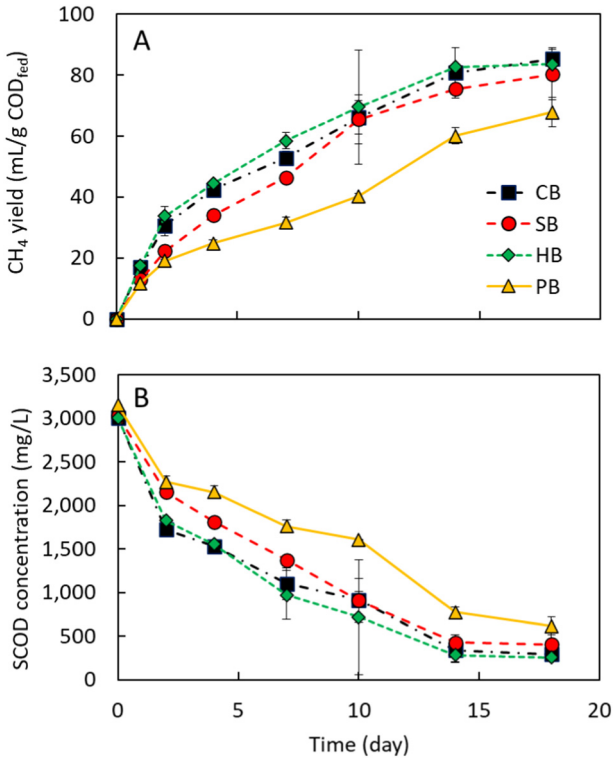

Fig. 2. (A) Methane production and (B) soluble COD degradation profiles during the fourth batch cycle.

for initial microbial attachment (Zhang et al., 2012). A previous study by Wang et al. (2019b) found that methane production in an AD-MEC was slower than that obtained using Ni or Cu-cathodes. The authors suggested poor biocompatibility of stainless steel surface and possible antibacterial element generation during the production process of stainless steel as the main reasons (Wang et al., 2019b). With replacement medium between every batch cycle, biomass that was acclimated under stainless steel-added condition could be largely washed out and thus microbial cells loosely attached to the brush fibers could be detached into the bulk solution (i.e., during the draw-and-fill process of 50% of the liquid volume). However, after day 7 the stainless steel brush reactor showed methane production and SCOD removals comparable to the carbon and horsehair brush reactors. Carbon fibers used here had an electrical conductivity of 6.5 S/m compared to that of 139 S/cm reported for stainless steel 304 used in this study (Mitchell, 2004). The use of electrically conductive materials in AD has been reported to enhance the methanogenic performance by stimulating DIET (Baek et al., 2018). The higher AD efficiency observed in the carbon and stainless steel brush reactors could be partially explained by their conductive surface. If electrical conductivity was the sole factor affecting AD performance, the stainless steel brush reactors should have had the best performance, followed by carbon brush, and the other two materials. However, non-conductive horsehair brushes showed comparable methanogenic efficiency to the two electrically conductive materials demonstrating that there must be other crucial factors that dictate AD performance other than only electrical conductivity.

3.2. VFA profiles

There was a rapid increase in VFA concentration in the initial period in all reactors with 18–29 mL of H_2 production (data not shown) along with a drop in pH (Fig. S3), indicating that acidogenesis by glucose fermentation actively occurred (Fig. 3). Compared to the carbon and horsehair brush reactors which showed immediate degradation of VFAs (primarily butyrate) after day 2, stainless steel and polyester brush

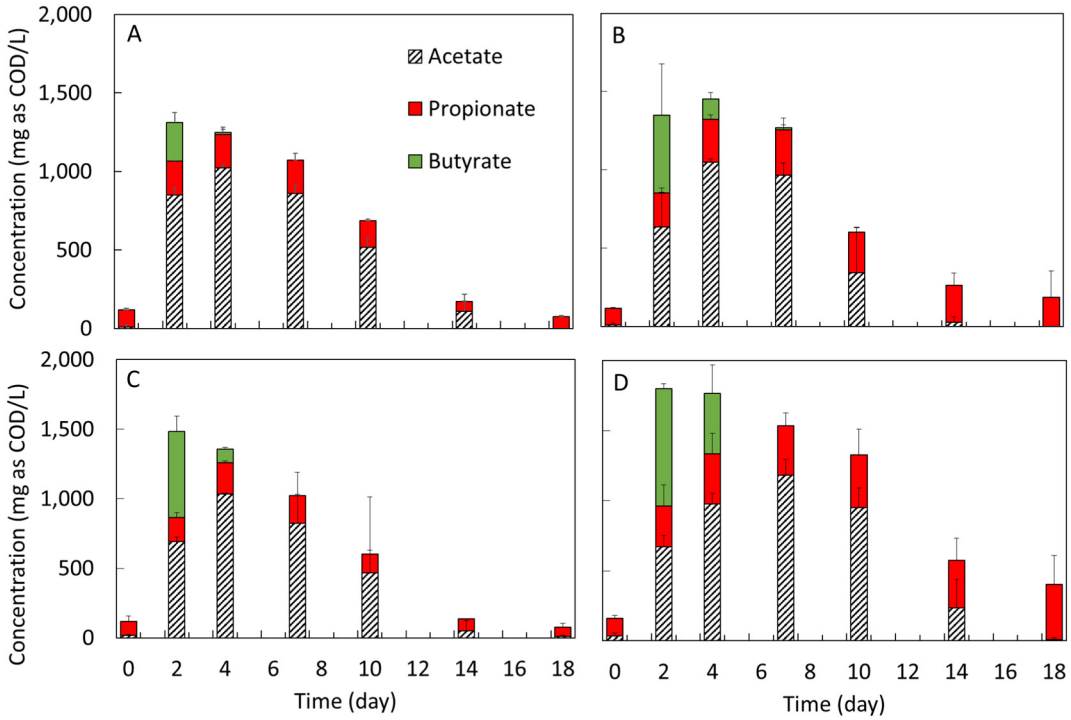

Fig. 3. Production and consumption profiles of acetate, propionate, and butyrate in (A) CB, (B) SB, (C) HB and (D) PB during the fourth batch cycle.

reactors showed only slight decrease (polyester) or even increase (stainless steel) of total VFAs, possibly due to a slower butyrate degradation. This observation suggests lower methanogenic rates in the initial period and/or slower acidogenesis rates for polyester and stainless steel brush reactors. Biomass retention inside the anaerobic reactors has been reported as a crucial factor in acidogenic fermentation rates (Bengtsson et al., 2008). Due to surface properties of stainless steel and polyester fibers, which were expected to have poor bioadhesion properties, acidogenesis from glucose might be less efficient compared to the other two materials. However, after day 7, stainless steel brush reactor showed VFA degradation rates comparable to those of the carbon and horsehair brush reactors while the polyester brush reactor maintained lower degradation rate of acetate and propionate. Butyrate was fully degraded in all reactors after day 7 and acetate was mostly consumed at the end of the experiment (<10 mg COD/L). Propionate was the only remaining VFAs in all reactors on the final day, but its concentration was much higher in the polyester brush reactor (403 ± 194 mg COD/L) than in the others (69–187 mg COD/L). Given that propionate oxidation is not thermodynamically favorable and requires obligate syntrophic relationship between microbial groups (De Bok et al., 2004), a more favorable environment for syntrophic degradation was likely developed in the reactors with brush materials other than polyester.

3.3. The impact of fiber characteristics on microbial attachment

To evaluate biocompatibility of the different materials, we examined the initial rates of VSS production and measured protein concentrations on the different brushes. Much higher VSS concentrations were measured in the effluent after each batch cycle using stainless steel and polyester brush reactors than other two during whole experimental period (Fig. 4A). Particularly during the initial two batch cycles, the VSS concentrations were 6–11 times (after the first cycle) and 2 times (after the second cycle) higher in stainless steel and polyester brush reactors than the other two fiber brushes, suggesting that biomass which was initially added into the medium was not effectively attached to the stainless steel and polyester fibers and would therefore be washed out when replenishing the medium. In contrast, the effluent of carbon and horsehair brush reactors contained only 200–700 mg/L of VSS after all the batch cycles showing good retention of the inoculum. The differences in VSS concentrations in the mixed liquor were consistent with

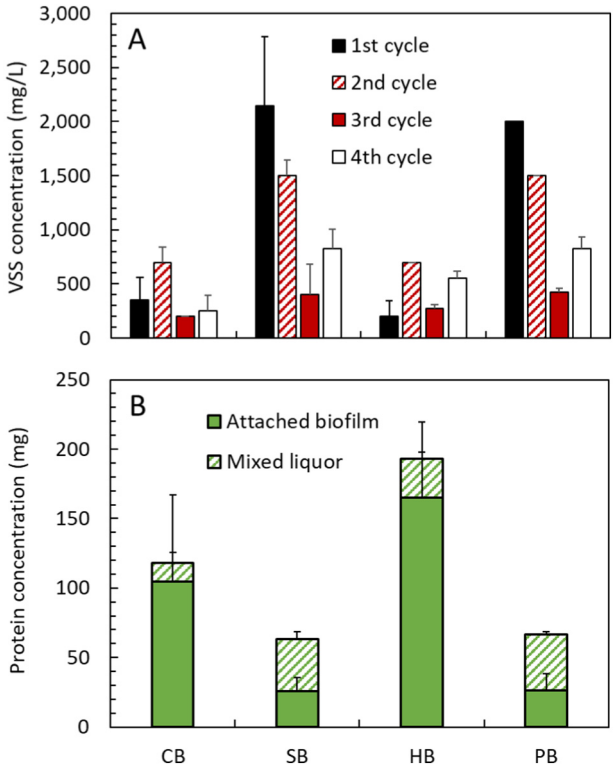

Fig. 4. (A) Volatile suspended solid (VSS) concentrations in the effluent at the end of each batch cycle and (B) protein concentrations of the biofilm attached to the fibers and mixed liquor at the end of the fourth batch cycle.

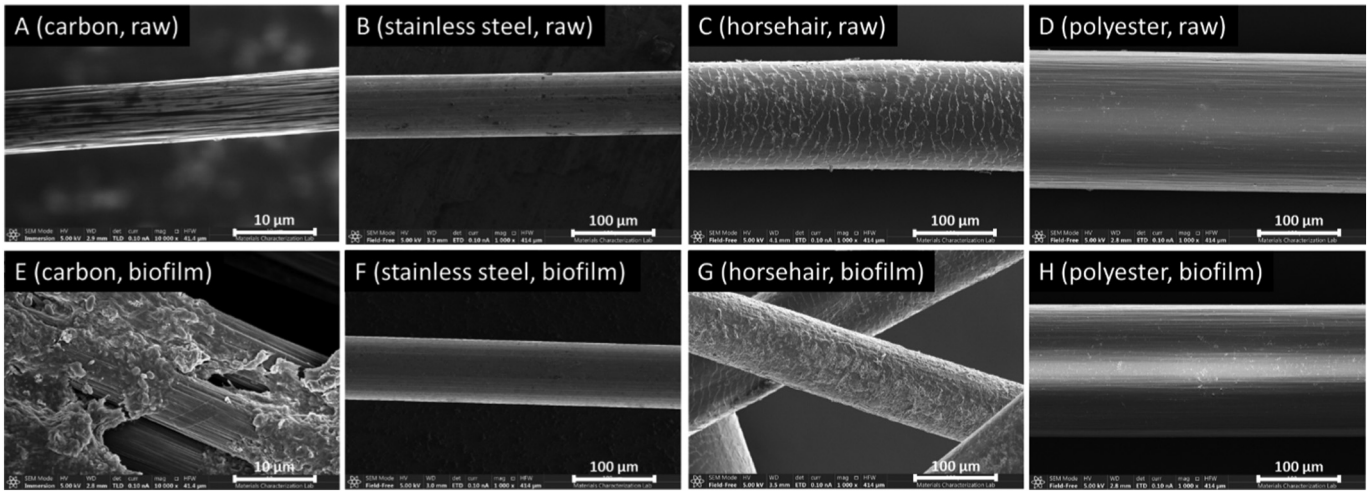

Fig. 5. Scanning electron microscopy images of the (A, B, C, and D) raw fibers and (E, F, G, and H) biofilm-covered fibers collected at the end of the experiment.

visual observations of the operating reactors during the first batch cycle (Fig. 1C).

Higher biomass attachment on carbon fiber and horsehair was shown based on protein measurements for biofilms on the brushes as well as in the mixed liquor (Fig. 4B). For the attached biofilms, much higher protein concentrations were obtained for the carbon and horsehair brushes (105–165 mg) than other two (26 ± 1 mg), while the concentration of protein in the mixed liquor was higher in stainless steel and polyester brushes reactors (38–40 mg) than other two (13–28 mg). Even though the same amount of inoculum was added into the reactors at the beginning of the experiments, the mixed liquor was much clearer with lower turbidity in carbon and horsehair brush reactors compared to the other two fiber brushes.

Biofilm formation on each fiber was examined by SEM, confirming much thicker and denser biofilms were formed on the surfaces of the carbon and horsehair fibers while little biofilm was found to be attached to the surfaces of stainless steel or polyester fibers (Fig. 5E, F, G, and H). It is known that the different characteristics of materials, such as roughness, wettability, and hydrophilicity, can impact biofilm formation (De Avila et al., 2016). As for the hydrophilicity, it has been previously reported that polyester has hydrophobic surface, stainless steel has mildly hydrophobic surface, and carbon fiber and horsehair have hydrophilic surfaces (Bajpai et al., 2011; Guillemot et al., 2006; Santoro et al., 2014; Tow et al., 2017). Highly hydrophilic property is typically beneficial for biofilm formation (Katuri et al., 2020), thus could impact AD efficiency positively in this study. In addition, highly rough surface structure was observed in raw carbon fiber and horsehair compared to smoother stainless steel and polyester surfaces (Fig. 5A, B, C, and D). Rough surface usually provides more suitable condition for biofilm development on the electrodes in microbial fuel cells (MFCs) while electrodes with smooth surface was reported to produce less power (Zhang et al., 2012).

3.4. Microbial community structure

Eight biomass samples were taken from the biofilms on brushes and the solutions in each reactor and analyzed for 16S rRNA to examine the active microbial populations. A total of 199,879 (rRNA library) non-chimeric, quality-filtered reads were obtained that were clustered into 298 OTUs with a 97% identity. The 20 most abundant OTUs in each library were examined in a heatmap with their relative abundance and taxonomic classification at the genus and phylum levels (Fig. 6), and family level (Fig. 7A).

In the archaeal community structure, highly enriched communities of *Methanosaeta* (acetoclastic methanogens), *Methanosarcina* (contains hydrogenotrophic and acetoclastic methanogens), *Methanofollis, Methanobrevibacter*, and *Methanobacterium* (hydrogenotrophic methanogens) were observed depending on the reactor environment, suggesting that the surface characteristics of material substantially impacted the methanogenic activity. *Methanosaeta* (OTU_12) was more abundant in the biofilm samples (2.3–5.0%) compared to those for the solution samples (0.2–2.0%). This might be because *Methanosaeta* prefer to grow in the biofilm because they can be retained much longer than in the suspension due to their slow growth rate (Conklin et al., 2006; Harb et al., 2015). *Methanosaeta* were more dominant in the biofilms on carbon and stainless steel brushes, compared to other two materials, suggesting that the electrical conductivity of the fiber surface might stimulate their growth. *Methanosaeta* are known acetoclastic methanogens but recently it was revealed that they can participate in DIET in the presence of conductive materials by directly reducing CO_2 to CH_4 via electromethanogenesis (Baek et al., 2020; Rotaru et al., 2014; Zhao et al., 2018). The highest abundance of *Methanosaeta* in both biofilm and solution samples in stainless steel brush reactor could be related to higher AD performance of stainless steel brush reactor than polyester brush reactor although, both have low biocompatible fiber surfaces. Furthermore their relative abundance was even higher in the biofilm of stainless steel than that of carbon fiber, which was likely due to the high electrical conductivity of stainless steel than carbon fiber used here. The relative abundance of hydrogenotrophic methanogens including genus *Methanofoliis* (OTU_11 and OTU_26), *Methanobrevibacter* (OTU_17), *Methanocorpusculum* (OTU_4), and *Methanobacterium* (OTU_21) was higher in the carbon and horsehair biofilm samples (5.0–5.4%) compared to the other two reactor samples (2.3–3.2%). High enrichment of hydrogenotrophic methanogens might help to maintain low H_2 concentrations in the digesters during fermentation and thus account for the improved AD performance observed in carbon and horsehair brush reactors (Fig. 2).

The bacterial communities in all samples were dominated by *Firmicutes* (51.8–67.5%), indicating their major role in overall microbial activities (Fig. 7B). The genus *Clostridium* sensu stricto *1* (OTU_1 and OTU_2) was responsible for high abundance of *Firmicutes* in all reactors (Fig. 6). This genus is known to produce acid from organic carbon substrates and its dominance has been reported in anaerobic digesters or fermenters fed with glucose, which was the substrate used here (Lu et al., 2020; Yang and Wang, 2019). The OTU_7, closely affiliated to genus *Petrimonas* were more abundant in carbon, stainless steel, and horsehair brush biofilms than polyester brush biofilm. *Petrimonas* might be responsible for the better performance of these three reactors by adhering to the fibers, given that they were reported to ferment glucose and they were more abundantly observed at biofilm of supporting

	Biofilm				Solution				
	CB	SB	HB	PB	CB	SB	HB	PB	
Methanosarcina; OTU_14	0.6	2.2	4.5	2.7	0.3	1.3	2.2	4.0	*Euryarcheota*
Methanofollis; OTU_11	1.9	0.1	1.3	0.3	9.1	1.6	1.2	1.1	
Methanosaeta; OTU_12	3.0	5.0	2.5	2.3	0.2	2.0	0.6	1.0	
Methanobrevibacter; OTU_17	2.2	1.0	0.5	0.6	1.1	1.8	0.5	1.2	
Methanocorpusculum; OTU_4	0.1	0.5	0.8	0.4	0.2	2.6	1.3	1.1	
Methanobacterium; OTU_21	0.3	0.6	0.8	1.3	0.4	1.4	0.6	1.1	
Methanofollis; OTU_26	0.6	0.0	2.0	0.5	0.5	0.1	0.4	1.0	
Clostridium sensu stricto 1; OTU_1	30.5	44.8	41.3	39.1	24.0	38.8	52.2	36.7	*Firmicutes*
Clostridium sensu stricto 1; OTU_2	21.8	5.8	1.7	17.6	31.0	5.3	1.5	16.3	
Clostridium sensu stricto 12; OTU_22	0.7	4.3	2.0	2.6	0.3	1.0	0.4	0.6	
Romboutsia; OTU_16	1.6	1.2	2.1	1.1	1.2	0.9	1.8	0.9	
Turicibacter; OTU_23	1.3	1.3	2.0	1.2	0.8	0.7	1.4	0.8	
f__Lentimicrobiaceae; OTU_5	4.6	10.1	3.6	6.5	0.9	5.6	1.4	5.2	*Bacteroidetes*
Petrimonas; OTU_7	1.6	1.1	2.0	0.8	5.0	1.9	1.5	2.4	
f__Lentimicrobiaceae; OTU_27	1.6	0.4	1.5	0.9	0.6	0.4	1.2	1.0	
Proteiniphilum; OTU_20	0.9	1.4	0.5	0.4	0.9	1.6	0.5	0.8	
Petrimonas; OTU_62	0.8	0.6	0.8	0.4	1.6	0.9	0.5	0.9	
f__Rhodocyclaceae; OTU_8	0.3	0.1	2.1	0.8	1.1	6.0	7.9	1.7	*Proteobacteria*
Candidatus Cloacimonas; OTU_9	1.7	1.2	2.5	1.5	5.1	1.9	2.1	2.2	*Cloacimonetes*
Desulfurella; OTU_25	1.1	0.8	1.7	2.3	0.4	1.3	0.8	1.4	*Epsilonbacteraeota*

Fig. 6. Heatmap of the relative abundance (%) of the top 20 dominant OTUs based on 16S rRNA analysis. The genus level or lowest taxonomic classification possible (f: family) are shown in the left column and the phylum levels are shown in the right column.

media (e.g., carbon cloth and polypropylene carriers) than solution in previous studies (Feng et al., 2020; Liu et al., 2017; Zhang et al., 2013).

Overall, the changes in community structure depending on the sampling point (i.e., biofilm or solution) in the same reactor were more obvious in archaeal community ($0.48 <$ Sorensen distance (D_S) < 0.73) than bacterial community ($0.74 < D_S < 0.88$), possibly due to slower growth rate of archaea than bacteria. This observation is in line with a previous study that reported the archaeal population is more

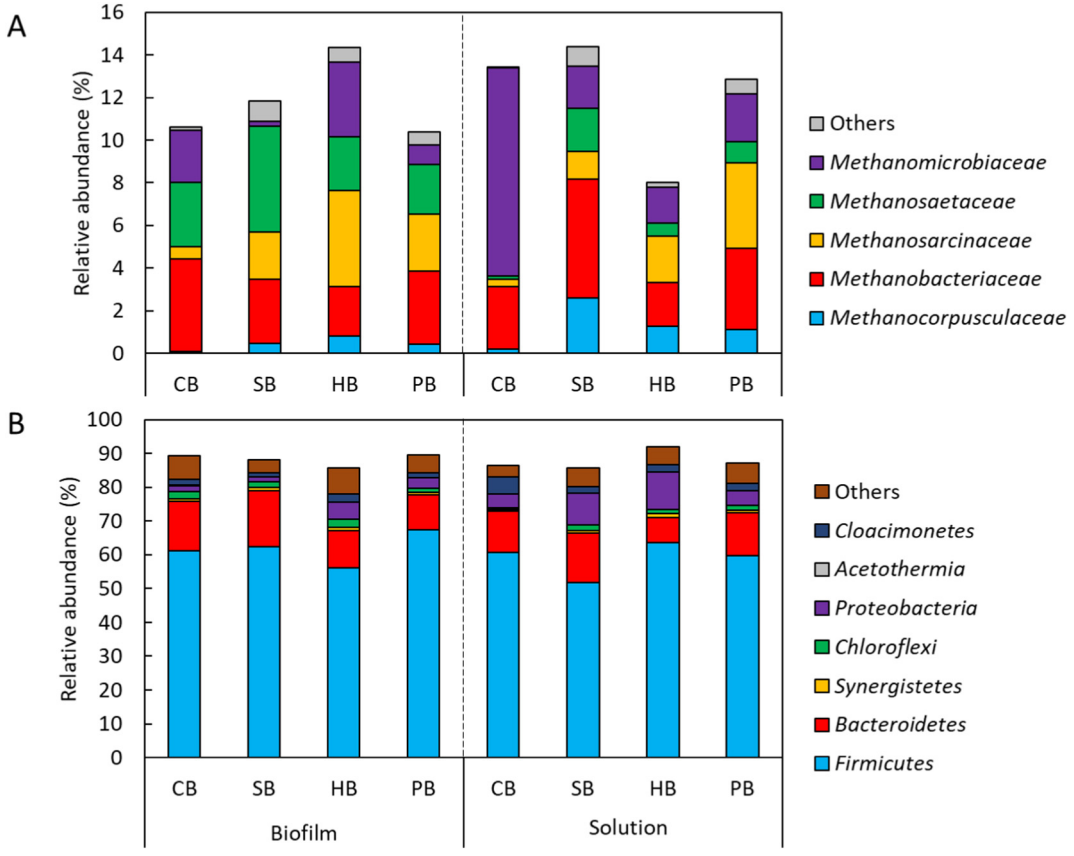

Fig. 7. The relative abundance of (A) methanogenic community at the family level and (B) bacterial community at the phylum level based on 16S rRNA analysis data. The community with relative abundance <1% (archaea) or < 5% (bacteria) of the sequence reads in all samples was classified as "Others".

highly dependent on support materials than bacterial population in lab-scale fixed-film reactors (Habouzit et al., 2014).

Despite of the differences in microbial community structures depending on the reactor environment (Figs. 6 and 7), it is difficult to find any obvious relationship between fiber characteristics and community structure. For example, even though both carbon and stainless steel brushes were electrically conductive materials, the biofilm microbial community structure that developed on both materials was substantially different (Fig. S4). This implies that the electrical conductivity was not the major factor in the difference of these microbial communities, and that other physicochemical characteristics of the materials were more important relative to AD performance. In addition, the relative abundances of several genera which were previously reported to be increased in DIET-stimulating condition (e.g., *Geobacter*, *Syntrophobacter*, *Syntrophomonas* and *Longilinea*) showed no significant difference between the samples with and without electrical conductivity (Fig. S5) (Lin et al., 2017; Wang et al., 2019a; Xing et al., 2020; Zhang et al., 2020). Even though the relative abundance of *Geobacter*, frequently reported as a representative DIET partner with electrotrophic methanogens, was 1.9-fold (biofilm samples) and 2.5-fold (solution samples) higher in carbon brush reactors than horsehair brush reactors, both reactors showed comparable AD efficiency. Therefore, there must have been additional factors that enhanced methane production than electrical conductivity. For example, better adhesion to the horsehair than the carbon or stainless steel could have impacted the absolute biomass concentration and thus the overall performance for methane generation (Fig. 4). The overall observation suggests that more careful consideration is needed to speculate on DIET stimulation only based on the comparison of AD performance and the relative abundances of electroactive microorganisms (e.g., *Geobacter*) between reactors with or without conductive materials.

3.5. Implications

Higher methane production rates observed from non-conductive horsehair-added reactors, as well as conductive carbon and stainless steel brush reactors compared to polyester brush reactors indicated that electrical conductivity was not a prerequisite for enhanced AD performance. The use of highly biocompatible materials (i.e., horsehair in this study) had methane production rates comparable to those using electrically conductive materials. This shows that a beneficial effect of high biomass retention by either high surface areas or highly biomass compatible materials on AD performance was not negligible in the previous conductive materials-induced DIET studies. The importance of biocompatibility can be supported by a previous study which compared the biofilm formation on the carbon fiber veil, carbon paper, graphite rod, and graphite foil as anode materials in MFCs (Liu et al., 2010). Although all of these carbon-based materials had similar electrical conductivity, biofilms formed much better on the carbon fiber veil and paper materials than the rod and foil, due to differences in surface properties. However, given that stainless steel brush reactors, which had low biomass retention also showed similar AD performance with carbon fiber and horsehair brush reactors, the benefits from the electrical conductivity may overcome the lower biofilm formation in these reactors.

The importance of the electrical conductivity relative to other factors in conductive materials-added AD has been previously reviewed by Martins et al. (2018). The authors noted that the mechanisms behind the effect of conductive materials might be related to more than one factor, and could be a complex relationship between electrical conductivity, redox potential, specific surface area, and roughness of the surface. Thus, they recommended one or more controls with non-conductive materials (Martins et al., 2018). Based on the results of the present study, however, the addition of a non-conductive material alone cannot serve as a proper control if the material has low biocompatibility for biomass retention. For example, horsehair reactors performed much better than those with polyester brushes despite of the fact that both materials were electrically insulative. In addition, the results of this study implies that polyester cloth was not a suitable control for as a non-electrically conductive material, although it has been used in several DIET studies as a control (Dang et al., 2016; Dang et al., 2017; Jia et al., 2020). Thus, it is recommended that the biocompatibility of the material be more carefully considered when conductive materials or non-conductive controls are used in AD reactors. The biocompatibility can be evaluated based on quantifying biomass attached to the materials when biomass is initially colonized (van Loosdrecht et al., 1990) and using surface characterization techniques such as SEM and contact angle measurements. In this study, we used SEM to observe the micro-scale structure of each fiber surface, but it was not possible to perform contact angle measurements due to the small diameter of some fibers ($<10^{-3}$ cm).

It is reasonable that much higher methane production could be obtained using carbon brushes than the other three materials due to the higher specific bristle areas of the carbon brushes (Fig. S1). However, biomass retention by the carbon brushes was similar or even lower than the horsehair brush (Fig. 4B). There was no evidence of a direct relationship between biomass retention and specific bristle area although the impact of mass of the brush was not examined here. Also, the carbon fibers tend to clump together so that the function area of the brushes might be less than the calculated area based on the mass of fibers (Fig. 5E). It was previously reported that an increase in specific surface area of carbon fibers did not linearly increase the AD efficiency and the authors suggest that the agglomeration of fibers could be a main reason (Barua et al., 2019). This observation implies that the chemical properties of fiber rather than just absolute quantity of surface area has more critical impact on microbial attachment.

4. Conclusions

The addition of electrically conductive carbon brushes to AD reactors was compared to the effects of brushes made of horsehair, polyester, and stainless steel. Among these four materials only the polyester brush reactors showed lower methane production and organic removal efficiencies than the others. The good performance of the non-electrically conductive horsehair brushes suggests that poor performance of the polyester was due more to its lack of compatibility for bioadhesion than electrically conductivity, and thus it may be a poor control in DIET studies. Biomass concentration was much higher in carbon and horsehair brush reactors than other two due to better biocompatibility for biomass retention using these two materials. The results of this study suggest that adding electrically conductive materials is not necessarily required to enhance AD performance and that other surface characteristics such as biocompatibility must also be also considered when choosing suitable controls for non-conductive materials in DIET studies.

Declaration of competing interest

The authors declare that they have no known competing financial interests or personal relationships that could have appeared to influence the work reported in this paper.

Acknowledgements

This research was funded by the Stan and Flora Kappe endowment and other funds through The Pennsylvania State University.

Appendix A. Supplementary data

Supplementary data to this article can be found online at https://doi.org/10.1016/j.scitotenv.2021.147683.

References

Al-Amshawee, S., Yunus, M.Y.B.M., Lynam, J.G., Lee, W.H., Dai, F., Dakhil, I.H., 2020. Roughness and wettability of biofilm carriers: a systematic review. Environ. Technol. Innov. 21, 101233.

Apprill, A., McNally, S., Parsons, R., Weber, L., 2015. Minor revision to V4 region SSU rRNA 806R gene primer greatly increases detection of SAR11 bacterioplankton. Aquat. Microb. Ecol. 75, 129–137.
Baek, G., Jung, H., Kim, J., Lee, C., 2017. A long-term study on the effect of magnetite supplementation in continuous anaerobic digestion of dairy effluent–magnetic separation and recycling of magnetite. Bioresour. Technol. 241, 830–840.
Baek, G., Kim, J., Kim, J., Lee, C., 2018. Role and potential of direct interspecies electron transfer in anaerobic digestion. Energies 11, 107.
Baek, G., Kim, J., Kim, J., Lee, C., 2020. Individual and combined effects of magnetite addition and external voltage application on anaerobic digestion of dairy wastewater. Bioresour. Technol. 297, 122443.
Baek, G., Saikaly, P.E., Logan, B.E., 2021. Addition of a carbon fiber brush improves anaerobic digestion compared to external voltage application. Water Res. 188, 116575.
Bajpai, V., Dey, A., Ghosh, S., Bajpai, S., Jha, M.K., 2011. Quantification of bacterial adherence on different textile fabrics. Int. Biodeterior. Biodegrad. 65, 1169–1174.
Barua, S., Zakaria, B.S., Lin, L., Dhar, B.R., 2019. Shaping microbial communities with conductive carbon fibers to enhance methane productivity and kinetics. Bioresour. Technol. Rep. 5, 20–27.
Bengtsson, S., Hallquist, J., Werker, A., Welander, T., 2008. Acidogenic fermentation of industrial wastewaters: effects of chemostat retention time and pH on volatile fatty acids production. Biochem. Eng. J. 40, 492–499.
Bian, B., Shi, D., Cai, X., Hu, M., Guo, Q., Zhang, C., et al., 2018. 3D printed porous carbon anode for enhanced power generation in microbial fuel cell. Nano Energy 44, 174–180.
Bond, D.R., Lovley, D.R., 2003. Electricity production by *Geobacter sulfurreducens* attached to electrodes. Appl. Environ. Microbiol. 69, 1548–1555.
Conklin, A., Stensel, H.D., Ferguson, J., 2006. Growth kinetics and competition between Methanosarcina and Methanosaeta in mesophilic anaerobic digestion. Water Environ. Res. 78, 486–496.
Dang, Y., Holmes, D.E., Zhao, Z., Woodard, T.L., Zhang, Y., Sun, D., et al., 2016. Enhancing anaerobic digestion of complex organic waste with carbon-based conductive materials. Bioresour. Technol. 220, 516–522.
Dang, Y., Sun, D., Woodard, T.L., Wang, L.-Y., Nevin, K.P., Holmes, D.E., 2017. Stimulation of the anaerobic digestion of the dry organic fraction of municipal solid waste (OFMSW) with carbon-based conductive materials. Bioresour. Technol. 238, 30–38.
De Avila, E.D., Avila-Campos, M.J., Vergani, C.E., Spolidório, D.M.P., de Assis Mollo Jr., F., 2016. Structural and quantitative analysis of a mature anaerobic biofilm on different implant abutment surfaces. J. Prosthet. Dent. 115, 428–436.
De Bok, F., Plugge, C., Stams, A., 2004. Interspecies electron transfer in methanogenic propionate degrading consortia. Water Res. 38, 1368–1375.
Feng, D., Xia, A., Liao, Q., Nizami, A.-S., Sun, C., Huang, Y., et al., 2020. Carbon cloth facilitates semi-continuous anaerobic digestion of organic wastewater rich in volatile fatty acids from dark fermentation. Environ. Pollut. 272, 116030.
Guillemot, G., Vaca-Medina, G., Martin-Yken, H., Vernhet, A., Schmitz, P., Mercier-Bonin, M., 2006. Shear-flow induced detachment of Saccharomyces cerevisiae from stainless steel: influence of yeast and solid surface properties. Colloids Surf., B 49, 126–135.
Habouzit, F., Hamelin, J., Santa-Catalina, G., Steyer, J.P., Bernet, N., 2014. Biofilm development during the start-up period of anaerobic biofilm reactors: the biofilm Archaea community is highly dependent on the support material. Microb. Biotechnol. 7, 257–264.
Harb, M., Xiong, Y., Guest, J., Amy, G., Hong, P.-Y., 2015. Differences in microbial communities and performance between suspended and attached growth anaerobic membrane bioreactors treating synthetic municipal wastewater. Environ. Sci. Water Res. Technol. 1, 800–813.
Illumina, I., 2015. 16S metagenomic sequencing library preparation, part# 15044223 Rev. B. pp. 1213–1214.
Ishii, Si, Watanabe, K., Yabuki, S., Logan, B.E., Sekiguchi, Y., 2008. Comparison of electrode reduction activities of Geobacter sulfurreducens and an enriched consortium in an air-cathode microbial fuel cell. Appl. Environ. Microbiol. 74, 7348–7355.
Jia, R., Sun, D., Dang, Y., Meier, D., Holmes, D.E., Smith, J.A., 2020. Carbon cloth enhances treatment of high-strength brewery wastewater in anaerobic dynamic membrane bioreactors. Bioresour. Technol. 298, 122547.
Katuri, K., Kamireddy, S., Kavanagh, P., Ali, M., Peter, C., Kumar, A., et al., 2020. Electroactive biofilms on surface functionalized anodes: the anode respiring behavior of a novel electroactive bacterium *Desulfuromonas acetexigens*. Water Res. 185, 116284.
Lei, Y., Sun, D., Dang, Y., Feng, X., Huo, D., Liu, C., et al., 2019. Metagenomic analysis reveals that activated carbon aids anaerobic digestion of raw incineration leachate by promoting direct interspecies electron transfer. Water Res. 161, 570–580.
Lin, R., Cheng, J., Zhang, J., Zhou, J., Cen, K., Murphy, J.D., 2017. Boosting biomethane yield and production rate with graphene: the potential of direct interspecies electron transfer in anaerobic digestion. Bioresour. Technol. 239, 345–352.
Liu, C., Yuan, X., Gu, Y., Chen, H., Sun, D., Li, P., et al., 2020a. Enhancement of bioelectrochemical CO_2 reduction with a carbon brush electrode via direct Electron transfer. ACS Sustain. Chem. Eng. 8, 11368–11375.
Liu, J., Liu, T., Chen, S., Yu, H., Zhang, Y., Quan, X., 2020b. Enhancing anaerobic digestion in anaerobic integrated floating fixed-film activated sludge (An-IFFAS) system using novel electron mediator suspended biofilm carriers. Water Res. 175, 115697.
Liu, Y., Harnisch, F., Fricke, K., Schröder, U., Climent, V., Feliu, J.M., 2010. The study of electrochemically active microbial biofilms on different carbon-based anode materials in microbial fuel cells. Biosens. Bioelectron. 25, 2167–2171.
Liu, Y., Niu, Q., Wang, S., Ji, J., Zhang, Y., Yang, M., et al., 2017. Upgrading of the symbiosis of *Nitrosomanas* and anammox bacteria in a novel single-stage partial nitritation–anammox system: nitrogen removal potential and microbial characterization. Bioresour. Technol. 244, 463–472.
van Loosdrecht, M.C., Norde, W., Lyklema, J., Zehnder, A.J., 1990. Hydrophobic and electrostatic parameters in bacterial adhesion. Aquat. Sci. 52, 103–114.
Lovley, D.R., 2017. Syntrophy goes electric: direct interspecies electron transfer. Annu. Rev. Microbiol. 71, 643–664.
Lu, J.-H., Chen, C., Huang, C., Lee, D.-J., 2020. Glucose fermentation with biochar-amended consortium: microbial consortium shift. Bioengineered 11, 272–280.
Martins, G., Salvador, A.F., Pereira, L., Alves, M.M., 2018. Methane production and conductive materials: a critical review. Environ. Sci. Technol. 52, 10241–10253.
McCune, B., Grace, J.B., Urban, D.L., 2002. Analysis of Ecological Communities. Vol 28. MjM Software Design, Gleneden Beach, OR.
Mitchell, B.S., 2004. An Introduction to Materials Engineering and Science for Chemical and Materials Engineers. John Wiley & Sons.
Najafpour, G., Zinatizadeh, A., Mohamed, A., Isa, M.H., Nasrollahzadeh, H., 2006. High-rate anaerobic digestion of palm oil mill effluent in an upflow anaerobic sludge-fixed film bioreactor. Process Biochem. 41, 370–379.
Park, J.-H., Park, J.-H., Seong, H.J., Sul, W.J., Jin, K.-H., Park, H.-D., 2018. Metagenomic insight into methanogenic reactors promoting direct interspecies electron transfer via granular activated carbon. Bioresour. Technol. 259, 414–422.
Poirier, S., Madigou, C., Bouchez, T., Chapleur, O., 2017. Improving anaerobic digestion with support media: mitigation of ammonia inhibition and effect on microbial communities. Bioresour. Technol. 235, 229–239.
Rotaru, A.-E., Shrestha, P.M., Liu, F., Shrestha, M., Shrestha, D., Embree, M., et al., 2014. A new model for electron flow during anaerobic digestion: direct interspecies electron transfer to *Methanosaeta* for the reduction of carbon dioxide to methane. Energy Environ. Sci. 7, 408–415.
Santoro, C., Guilizzoni, M., Baena, J.C., Pasaogullari, U., Casalegno, A., Li, B., et al., 2014. The effects of carbon electrode surface properties on bacteria attachment and start up time of microbial fuel cells. Carbon 67, 128–139.
Tow, K.H., Chow, D.M., Vollrath, F., Dicaire, I., Gheysens, T., Thévenaz, L., 2017. Exploring the use of native spider silk as an optical fiber for chemical sensing. J. Lightwave Technol. 36, 1138–1144.
Wang, C., Liu, Y., Wang, C., Xing, B., Zhu, S., Huang, J., et al., 2021. Biochar facilitates rapid restoration of methanogenesis by enhancing direct interspecies electron transfer after high organic loading shock. Bioresour. Technol. 320, 124360.
Wang, C., Qiao, W., Chen, H., Xu, X., Zhu, L., 2019a. A short-term stimulation of ethanol enhances the effect of magnetite on anaerobic digestion. Appl. Microbiol. Biotechnol. 103, 1511–1522.
Wang, L., He, Z., Guo, Z., Sangeetha, T., Yang, C., Gao, L., et al., 2019b. Microbial community development on different cathode metals in a bioelectrolysis enhanced methane production system. J. Power Sources 444, 227306.
WEF AA, 2005. Standard Methods for the Examination of Waterand Wastewater. 21st edition. American Public Health Association, AmericanWater Works Association, Water Environmental Federation, Washington DC, USA.
Xing, L., Wang, Z., Gu, M., Yin, Q., Wu, G., 2020. Coupled effects of ferroferric oxide supplement and ethanol co-metabolism on the methanogenic oxidation of propionate. Sci. Total Environ. 723, 137992.
Yan, P., Zhao, Y., Zhang, H., Chen, S., Zhu, W., Yuan, X., et al., 2020. A comparison and evaluation of the effects of biochar on the anaerobic digestion of excess and anaerobic sludge. Sci. Total Environ. 736, 139159.
Yang, G., Wang, J., 2019. Changes in microbial community structure during dark fermentative hydrogen production. Int. J. Hydrogen Energ. 44, 25542–25550.
Yang, Y., Tada, C., Tsukahara, K., Sawayama, S., 2004. Methanogenic community and performance of fixed-and fluidized-bed reactors with reticular polyurethane foam with different pore sizes. Mater. Sci. Eng. C 24, 803–813.
Yin, Q., Wu, G., 2019. Advances in direct interspecies electron transfer and conductive materials: Electron flux, organic degradation and microbial interaction. Biotechnol. Adv. 37, 107443.
Yuan, H., Dong, G., Li, D., Deng, L., Cheng, P., Chen, Y., 2018. Steamed cake-derived 3D carbon foam with surface anchored carbon nanoparticles as freestanding anodes for high-performance microbial fuel cells. Sci. Total Environ. 636, 1081–1088.
Zhang, J., Zhang, Y., Quan, X., Chen, S., Afzal, S., 2013. Enhanced anaerobic digestion of organic contaminants containing diverse microbial population by combined microbial electrolysis cell (MEC) and anaerobic reactor under Fe(III) reducing conditions. Bioresour. Technol. 136, 273–280.
Zhang, J., Zhang, R., Wang, H., Yang, K., 2020. Direct interspecies electron transfer stimulated by granular activated carbon enhances anaerobic methanation efficiency from typical kitchen waste lipid-rapeseed oil. Sci. Total Environ. 704, 135282.
Zhang, M., Ma, Y., Ji, D., Li, X., Zhang, J., Zang, L., 2019. Synergetic promotion of direct interspecies electron transfer for syntrophic metabolism of propionate and butyrate with graphite felt in anaerobic digestion. Bioresour. Technol. 287, 121373.
Zhang, Y., Sun, J., Hu, Y., Li, S., Xu, Q., 2012. Bio-cathode materials evaluation in microbial fuel cells: a comparison of graphite felt, carbon paper and stainless steel mesh materials. Int. J. Hydrogen Energ. 37, 16935–16942.
Zhao, Z., Zhang, Y., Holmes, D.E., Dang, Y., Woodard, T.L., Nevin, K.P., et al., 2016. Potential enhancement of direct interspecies electron transfer for syntrophic metabolism of propionate and butyrate with biochar in up-flow anaerobic sludge blanket reactors. Bioresour. Technol. 209, 148–156.
Zhao, Z., Li, Y., Yu, Q., Zhang, Y., 2018. Ferroferric oxide triggered possible direct interspecies electron transfer between Syntrophomonas and Methanosaeta to enhance waste activated sludge anaerobic digestion. Bioresour. Technol. 250, 79–85.